

Alma Mater Studiorum Università di Bologna
Archivio istituzionale della ricerca

Gold(I)-Catalyzed Dearomative [2+2]-Cycloaddition of Indoles with Activated Allenes: A Combined Experimental-Computational Study

This is the final peer-reviewed author's accepted manuscript (postprint) of the following publication:

Published Version:

Gold(I)-Catalyzed Dearomative [2+2]-Cycloaddition of Indoles with Activated Allenes: A Combined Experimental-Computational Study / Ocello, Riccardo; DE NISI, Assunta; Jia, Minqiang; Yang, Qing Qing; Monari, Magda; Giacinto, Pietro; Bottoni, Andrea; Miscione, GIAN PIETRO; Bandini, Marco. - In: CHEMISTRY. - ISSN 1521-3765. - STAMPA. - 21:(2015), pp. 18445-18453. [10.1002/chem.201503598]

Availability:

This version is available at: <https://hdl.handle.net/11585/531933> since: 2020-02-22

Published:

DOI: <http://doi.org/10.1002/chem.201503598>

Terms of use:

Some rights reserved. The terms and conditions for the reuse of this version of the manuscript are specified in the publishing policy. For all terms of use and more information see the publisher's website.

This item was downloaded from IRIS Università di Bologna (<https://cris.unibo.it/>).
When citing, please refer to the published version.

(Article begins on next page)

This is the final peer-reviewed accepted manuscript of:

Gold(I)-Catalyzed Dearomative [2+2]-Cycloaddition of Indoles with Activated Allenes: A Combined Experimental–Computational Study

Chem.Eur.J. 2015, 21, 18445 – 18453

The final published version is available online at: **doi.org/10.1002/chem.201503598.**

Rights / License:

The terms and conditions for the reuse of this version of the manuscript are specified in the publishing policy. For all terms of use and more information see the publisher's website.

This item was downloaded from IRIS Università di Bologna (<https://cris.unibo.it/>)

When citing, please refer to the published version.

Gold(I)-Catalyzed Dearomative [2+2]-Cycloaddition of Indoles with Activated Allenes: A Combined Experimental–Computational Study

Riccardo Ocello,^[a] Assunta De Nisi,^[a] Minqiang Jia,^[b] Qing-Qing Yang,^[a] Magda Monari,^[a] Pietro Giacinto,^[a] Andrea Bottoni,^[a] Gian Pietro Miscione,^{*,[a, c]} and Marco Bandini^{*,[a]}

Abstract: The gold-catalyzed synthesis of methyldene 2,3-cyclobutane-indoles is documented through a combined experimental/computational investigation. Besides optimizing the racemic synthesis of the tricyclic indole compounds, the enantioselective variant is presented to its full extent. In particular, the scope of the reaction encompasses both arylox-yallenes and allenamides as electrophilic partners providing high yields and excellent stereochemical controls in the de-

sired cycloadducts. The computational (DFT) investigation has fully elucidated the reaction mechanism providing clear evidence for a two-step reaction. Two parallel reaction pathways explain the regioisomeric products obtained under kinetic and thermodynamic conditions. In both cases, the dearomative C–C bond-forming event turned out to be the rate-determining step.

Introduction

Achieving chemical complexity in indolyl-based alkaloid chemistry is currently attracting much interest in synthetic organic chemistry.^[1] In particular, the intrinsic molecular diversity of synthetic and natural occurring compounds belonging to this family continues to inspire developments in organic synthesis. To this aim, catalysis is the ultimate forefront in this area with a large portfolio of reliable metal- and metal-free methodologies available.^[2]

Partially dearomatized C(2),C(3)-polycyclic fused indoline and indolenine motifs are widely diffused molecular architectures in indole alkaloids, featuring stereochemically defined all-carbon quaternary stereocenters at the C(3)-position.^[3] A collection of titled compounds is shown in Figure 1.

Among the numerous catalytic methodologies available, the enantioselective C(2),C(3)-annulation of indoles by cycloaddi-

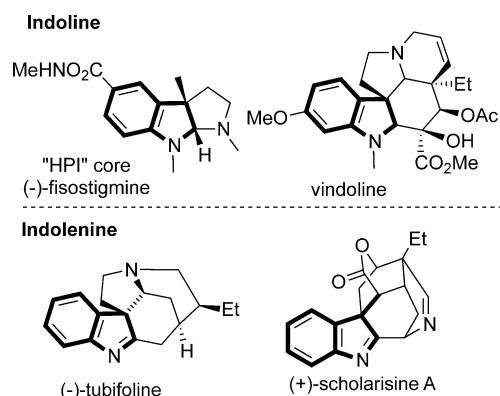


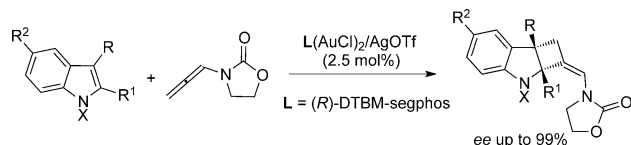
Figure 1. Collection of natural products featuring polycyclic C(2),C(3)-fused indoline and indolenine scaffolds.

tion reactions is gaining growing credit in terms of chemical efficiency. Based on these methodologies, densely functionalized C(2),C(3)-fused cyclopropane-([2+1]),^[4a] cyclopentane-([3+2])^[4b] and cyclohexa-indoline cores ([3+3])^[4c] have been prepared in a stereochemically defined manner.

Intriguingly, C(2),C(3)-indolincyclobutanes^[5] have found less attention in the literature. More precisely, besides the elegant intramolecular approach reported by Zhang,^[6a] the cyclobutyl-fused indole species was isolated in low yields through condensation of allenamides with indoles by Lopéz and Mascareñas.^[6b] Additionally, Xie and co-workers very recently documented the dearomative [2+2]-cycloaddition between *o*-carbonyne and *N*-silylated indoles under thermal conditions.^[7]

In this context, gold catalysis^[8] offers unique opportunities due to the peculiar characteristics of this coinage metal in pro-

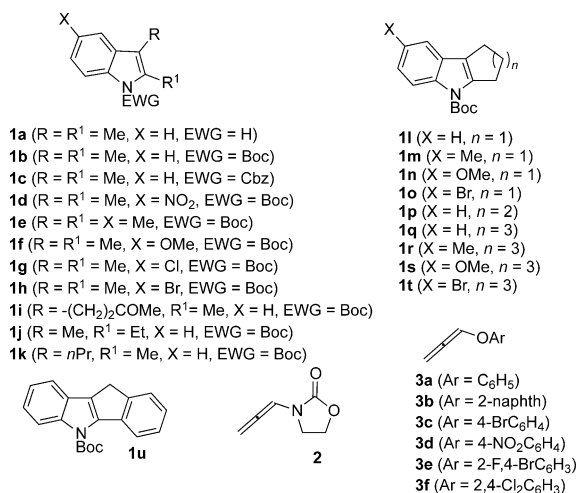
moting cycloaddition transformations through electrophilic activation of π -systems.^[9,10] Recently, we exploited the potential of gold-based catalysis and we documented the first enantioselective gold-catalyzed synthesis of C(2),C(3)-indolincyclobutanes by formal [2+2]-cycloaddition reactions between N-protected indoles and allenamides (Scheme 1).^[11]



Scheme 1. Preliminary results on the gold-catalyzed asymmetric condensation of indoles and allenamides.

In conjunction with our research interests focused on gold-assisted manipulation of indole rings,^[12] we present here a comprehensive investigation on the dearomative formal [2+2]-cycloaddition reaction between 2,3-disubstituted indoles and allenamides, to give densely functionalized 2,3-cyclobutyl-indolines. In particular, the gold-catalyzed racemic and enantioselective condensations of allenamide/aryloxyallenes with a range of N-substituted indoles **1** will be discussed. Moreover, a detailed computational investigation at the density functional theory (DFT) level is carried out to obtain a mechanistic insight on the high regioselectivity experimentally observed.

The complete range of indoles (**1**) and allenyl-derivatives (**2** and **3**) herein employed is shown below.



Results and Discussion

Gold-catalyzed dearomatization reaction: the racemic version (allenamides)

To optimize the synthesis of indolyl-2,3-cyclobutyl derivatives by cycloaddition reaction between electron-rich allenes and indoles, we examined initially a range of cationic [Au⁺] complexes in the model reaction involving the nitrogen-free 2,3-(Me)₂-indole **1a** and the allenamide **2**. At the same time, a survey of

reaction conditions showed DCM to be the best reaction medium.^[13] Initial attempts afforded the partially dearomatized indolenine **5a** and the nitrogen-allylated indole **6a** as main by-products of the process.

From the collection of results summarized on Table 1, [JohnPhosAu(NCMe)]SbF₆^[14] clearly emerged as a suitable catalyst in promoting the cycloaddition, providing the [2+2]-adduct **4a** as the major product (entry 6, yield 49%) under mild reaction conditions (CH₂Cl₂, RT, 16 h).

Table 1. Optimization of the reaction conditions for the racemic variant of the formal [2+2]-cycloaddition reaction.^[a]

Run	[Au] (5 mol %)	Yield [%] 4 ^[b]	Yield [%] ^[b] 5a/6a
1	JackiePhosAuNTf ₂	< 5 (4a)	22/33
2	Ph ₃ PAuNTf ₂	6 (4a)	18/75
3	XPhosAuNTf ₂	19 (4a)	—/—
4	JohnPhosAuTFA	< 5 (4a)	77/< 5
5	XPhosAuTFA	8 (4a)	70/< 5
6	[JohnPhosAu(NCMe)]SbF ₆	49 (4a)	5/—
7	[JohnPhosAu(NCMe)]SbF ₆	60 (4b)	—/—
8 ^[c]	[JohnPhosAu(NCMe)]SbF ₆	73 (4b)	—/—
9 ^[d]	[JohnPhosAu(NCMe)]SbF ₆	89 (4b)	—/—

[a] All the reactions were carried out under nitrogen atmosphere (1/2/[Au] = 1.2:1:0.05). [b] Isolated yields after flash chromatography. [c] T = −20 °C, t = 5 h. [d] T = −40 °C, t = 16 h.

Based on these promising results we inferred that the introduction of an electron-withdrawing group at the N-(1)-position of the indole could have significant effects on the reaction mechanism and its energetics by preventing the undesired N-alkylation (**6a**) and by increasing the electrophilic character of the intermediate immonium derivative (vide infra for further mechanistic details).^[15] We proved that, N-(Boc)-2,3-(Me)₂-indole **1b** is a competent reaction partner providing the desired diastereomerically pure cyclobutyl derivative **4b** in 60, 73 and 89% yield at room temperature, −20 and −40 °C, respectively (entries 7–9 of Table 1).^[16] The increase of isolated yields at lower temperatures can be rationalized in terms of minimization of gold-promoted self-condensation of **2** (i.e., dimerization or polymerization).^[10f]

Concerning the stereochemical aspects, optimal conditions provided the *cis*-C(2),C(3)-fused tricyclic compounds in high diastereomeric ratio (d.r. = 20:1). Furthermore, the *exo*-carbon=carbon double bond was exclusively obtained in the *Z* configuration.

The scope of the reaction was then examined by treating a range of N-protected-2,3-disubstituted indoles (**1c–u**) under the chosen conditions and the obtained results are collected in

Table 2. Interestingly, the cycloadducts **4c–k** were obtained in high yield from indoles carrying acyclic C(2),C(3) substituents (**1c–k**). Similarly, the presence of C5- and C7-membered cycles fused at the C(2),C(3)-positions of the pyrrolyl ring were adequately tolerated, providing the corresponding tetra- and pentacyclic compounds **4l–u** from moderate to excellent yields (41–95 %). This screening addressed also the tolerance towards substituents on the benzene ring. In particular, electron-donating (i.e., Me, OMe) and moderately electron-withdrawing groups (i.e., Br) were found to be effective in the process. On the contrary, strong EWG NO₂ group (C(5), **1d**) completely suppressed the kinetics of the transformation (entry 2). Finally, the Boc-protecting group was also successfully replaced by Cbz (**1c**) with an untouched isolated yield (95 %).

It is worth mentioning that, the 2,3-disubstitution pattern at the indole core was mandatory for the reaction. More precisely, while with *N*-Boc-indole and *N*-Boc-3-Me-indole the dimerization products of **2** were the main outcomes, *N*-Boc-2-Me-indole furnished the desired [2+2]-cycloadduct only in 18 % yield.

Gold-catalyzed dearomatization reaction: the racemic version (aryloxyallene)

Aryloxyallenes are an important class of electron-rich π -system that have found extensive application in organic chemistry, particularly with respect to cycloaddition reactions and site-selective condensation with nucleophilic agents.^[17] Analogously to the afore-described allenamides, the nucleophilic addition to the γ -carbon would lead to a formal allylation reaction with the simultaneous insertion of a synthetically versatile enol ether moiety.

Despite their undoubted synthetic interest, to the best of our knowledge, this family of unsaturated compounds has not been employed in dearomative processes to date.

To assess the possibility of extending this synthetic methodology to aryloxyallenes, a range of allenyl derivatives (**3a–f**)^[18] was synthesized through a conventional two-step procedure (i.e., propargylation of the corresponding phenol followed by base-assisted isomerization) and subjected to the dearomative cyclization in the presence of **1b** and [JohnPhosAu(NCMe)]SbF₆ (1–5 mol%).

The synthetic procedure turned out to be extraordinarily adaptable to a variety of aryloxyallenes. Accordingly, a range of racemic methylene cyclobutanes **7** (Table 3) was isolated as a single stereoisomer in good to excellent yields (75–96 %) under mild reaction conditions ([Au]: 1–5 mol%, DCM, 0 °C, 4 h).

Subsequently, the substrate scope was further investigated by condensing differently substituted *N*-Boc-indoles and allenenes **3b** and **3d**. The results reported in Scheme 2 emphasize the efficiency of the above-described gold-catalyzed methodology in providing densely functionalized tricyclic fused indolinyl scaffolds **7**.

In particular, we found that the reaction proved to be not significantly affected by the presence of substituents (including either carbon- or heteroatom-based groups) at the indole N(1),

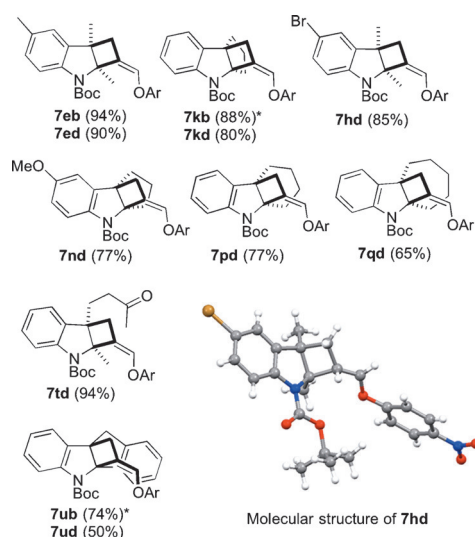
Table 2. Indole scope of the dearomative [2+2]-cycloaddition.^[a]

Run	1	Product (4)	Yield [%] ^[b]
1	1c	4c	95
2	1d	4d	n.r.
3	1e	4e	76
4	1f	4f	85
5	1j	4j	64
6	1k	4k	62
7	1l	4l	78
8	1m	4m	75
9	1n	4n	80
10	1o	4o	60
11	1q	4q	81
12	1r	4r	70
13	1s	4s	70
14	1t	4t	41

C(2), C(3) and C(5) positions. The isolated yields ranged between 50 and 94 % and the decrease of the catalyst loading to 1 mol % did not at all affect the chemical outcome. Both mo-

Table 2. (Continued)			
Run	1	Product (4)	Yield [%] ^[b]
15	1 u		95
[a] All the reactions were carried out under nitrogen atmosphere [Au]: [JohnPhosAu(NCMe)]SbF ₆ (5 mol %). [b] Isolated yields after flash chromatography. Each compound was isolated as a single diastereoisomer. n.r. = no reaction.			

Table 3. Gold-catalyzed dearomative [2+2]-cycloaddition between 1 a and aryloxyallenes 3. ^[a]			
Run	[Au] (x mol %)	3 (Ar)	Yield 7 [%] ^[b]
1	5	3 a (Ph)	75 (7 ba)
2	1	3 b (β-naphth)	83 (7 bb)
3	5	3 c (pBrC ₆ H ₄)	96 (7 bc)
4	5	3 d (pNO ₂ C ₆ H ₄)	81 (7 bd)
5	5	3 e (pF ₃ O-BrC ₆ H ₃)	83 (7 be)
6	5	3 f (p,o-Cl ₂ C ₆ H ₃)	95 (7 bf)
[a] All the reactions were carried out under nitrogen atmosphere (1 b/3 = 1.2:1). ^[b] Isolated yields after flash chromatography. d.r. > 20:1.			

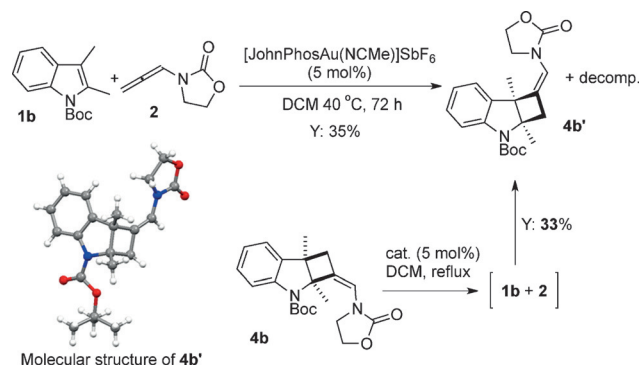


Scheme 2. Formal [2+2]-cycloaddition between *N*-Boc-indoles and aryloxyallenes (1 b/[JohnPhosAu(NCMe)]SbF₆ = 1.2:0.05, DCM, 0 °C, 16 h). *: 1 mol % of catalyst was used. All the compounds were obtained in racemic manner. 7xb: Ar = 2-naphth; 7xd: Ar = pNO₂C₆H₄.

lecular skeleton and stereochemical aspects were finally substantiated by obtaining the X-ray structure of (+/–)-7hd by slow evaporation from a solution of AcOEt.

Gold-catalyzed dearomatization reaction: mechanistic study

Interesting and unexpected experimental evidence was obtained on the classic cycloaddition reaction between allenamide 2 and NBoc-indole 1b. In particular, we observed that, when the condensation was carried out at temperatures higher than 0 °C (i.e., room temperature or 40 °C), we detected a second product that became predominant in the latter case (yield 35%). Crystallographic analysis showed that this product has the structure of the regioisomeric indoline-cyclobutyl ring 4b', corresponding to a reverse approaching orientation (with respect to 4b) of the two reaction partners (Scheme 3). Furthermore, when 4b was treated in the presence of the gold complex in hot DCM (40 °C), 4b' was again isolated along with some decomposition products. This experimental finding suggests the existence of a kinetic (4b) and thermodynamic (4b') product that can interconvert.

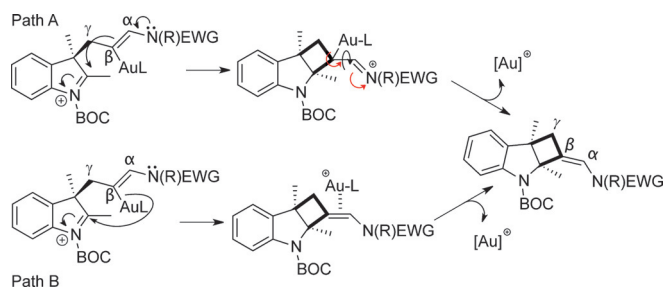


Scheme 3. Regiodivergent outcome of the [2+2]-cycloaddition when performed in refluxing DCM. Proving the interconversion of 4b into 4b' in hot DCM.

These intriguing experimental results stressed the importance of elucidating the reaction mechanism to answer important and unsolved questions, such as: 1) What is the coordination/activation mode of the gold catalyst with the allenamides?^[18] 2) Is the mechanism concerted or step-wise? 3) What is the rationale for the recorded regio- and stereochemistry? In particular, why does the ring closure occur without affecting the stereochemistry of the exocyclic double bond (Scheme 4)? 4) Are the “kinetic” and “thermodynamic” adducts the results of two separate reaction channels coexisting on the reaction surface?

To answer these questions we carried out a computational investigation of the reaction surface. We used a DFT approach and a model system formed by 1b and 2 activated by the [Au]⁺ cation bonded to the JohnPhos ligand ([JohnPhosAu]⁺).

First we examined how the cationic gold complex governs the electrophilic activation of allenamide 2.^[19] We found that the interaction of the metal with the cumulated diene involves



Scheme 4. Hypothetical mechanisms for the ring-closing step.

an equilibrium between three different complexes **M1**(π), **M2**(σ), **M3**(π) showing η^2 , η^1 and η^2 coordination to $[\text{Au}]^+$, respectively. Both η^2 complexes (**M1**(π) and **M3**(π)) are more stable than **M2**(σ) (2.9 and 3.4 kcal mol⁻¹, respectively; a 3D representation of the three complexes is given in Figure 2).

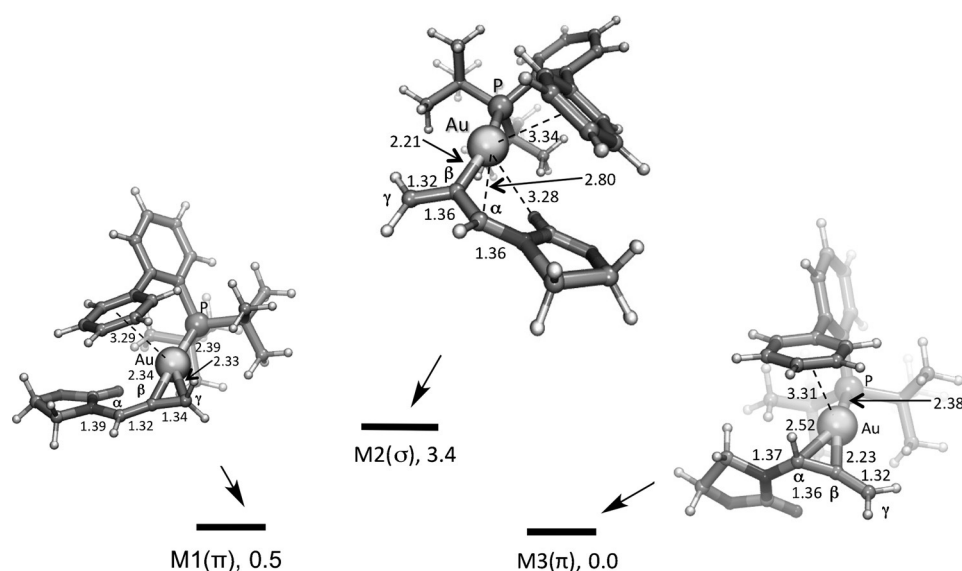


Figure 2. A schematic 3D representation of the allenamide- $[\text{Au}]^+$ complexes. Total energy values [kcal mol⁻¹] are relative to **M3**(π). Bond lengths are given in Å.

The perturbation of the π -system caused by the interaction with the gold complex is evidenced by a slight increase of the C–C bond lengths in **M1**(π) and **M3**(π) and the increase of the corresponding positive charge density on α and γ carbons.

The reaction surface for the cycloaddition involving indole **1b** and allenamide **2** complexed with $[\text{Au}]^+$ (reactants) is reported in Figure 3 where two reaction channels are evidenced. In the Figure a schematic representation of the corresponding reaction patterns is also given. Additionally, two-dimensional pictures of the structure of the various critical points located along the two pathways are given in Figure 4. More detailed 3D representations for each point are reported in Figures S1–S9 in the Supporting Information.

The approach of the two reacting species initially leads to the formation of an encounter complex **M0** (12.9 kcal mol⁻¹

more stable than reactants), where the indole ring plane and the plane of the metal allyl cation are facing each other, the C(3)–C γ and C(2)–C γ distances being 2.87 and 3.00 Å, respectively. Interestingly, in the encounter complex the preferred coordination of the gold cation is η^1 and not η^2 as found in the isolated allenamide- $[\text{JhonPhosAu}]^+$ species. The higher stability of the σ type complex (η^1) can be reasonably ascribed to the stabilizing interaction between the electron-rich indole π -system and the positive charge localized on the α allenamide carbon (0.3 is the net computed charge on C α).

Two reaction paths (both consisting of two steps) originate from **M0** and lead to different regioisomers corresponding to opposite approaching orientations of the reacting species (see above). These regioisomers should correspond to the hypothesized thermodynamic and kinetic products **4b'** and **4b** (the former being 3.5 kcal mol⁻¹ more stable than the latter). We denote the two paths leading to **4b'** and **4b** as Path(T) and Path(K), respectively.

Along Path(K) (kinetic pathway) the transition state **TS1**(K) (6.3 kcal mol⁻¹ above **M0**) corresponding to the rate-determining step of the process, describes the attack of C(3) on C γ and leads to the formation of the indoleninic intermediate **M1**(K), 13.6 kcal mol⁻¹ more stable than reactants. The newly forming bond is 2.17 Å in **TS1**(K) and becomes 1.57 Å in **M1**(K) where the bond formation is completed. Here the distance C(2)–C β (that identifies the second bond required to obtain the final product) is 2.73 Å. The σ -coordination of the gold atom as found in **M0** is conserved in **TS1**(K) and **M1**(K). The variation of the N–C(2) bond length along the transformation **M0**→**TS1**(K)→**M1**(K) (1.41, 1.37, 1.32 Å, respectively) indicates that the formation of the new C(3)–C γ bond is brought about by the indole nitrogen lone pair through an enaminic-type electronic shift (see **M1**(K) structure in Figure 4).

A rather low activation barrier (2.8 kcal mol⁻¹) must be overcome (transition state **TS2**(K)) to close the ring. The structure of **TS2**(K) is similar to that of the previous intermediate **M1**(K): the most important difference is the decrease of the C(2)–C β distance (the incipient C–C bond), which becomes 2.26 Å.

Importantly, the C α –C β bond length remains approximately constant on passing from **M1**(K) to **TS2**(K) (1.34 and 1.36 Å, respectively). This suggests that the formation of the C(2)–C β bond involves the $[\text{Au}]$ –C β heterolytic bond breakage (path B in Scheme 4) rather than the enamidic fragment (N–C α –C β) electrons (path A in Scheme 4). Thus, the ring-closing process does not affect the nature of the C α –C β exocyclic double

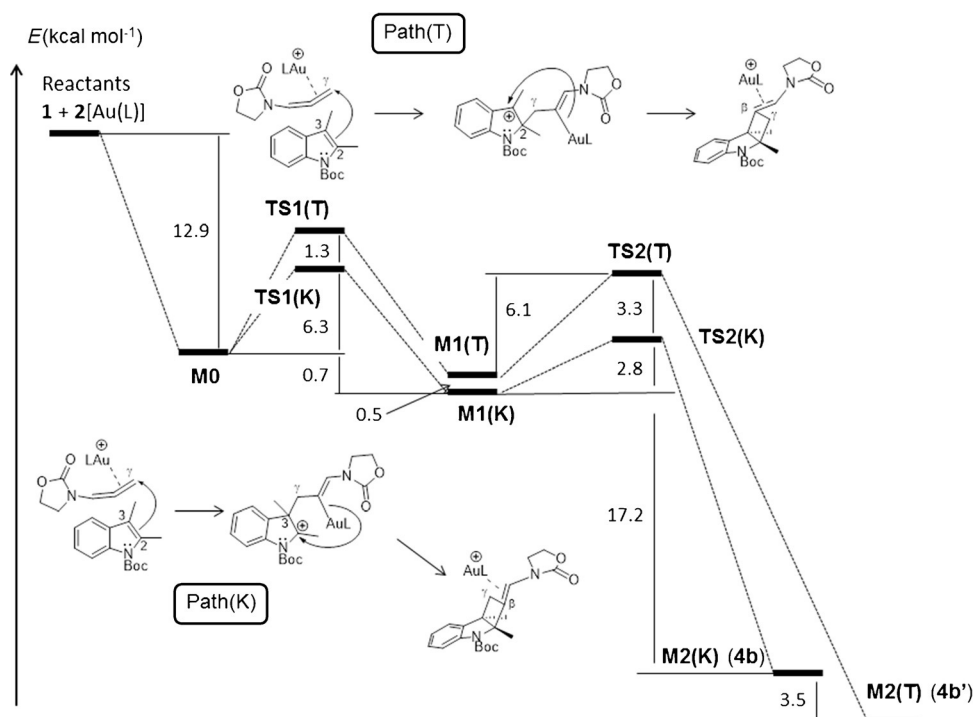


Figure 3. The two computed reaction profiles Path(K) and Path(T). The total energy values (E , kcal mol⁻¹) include ZPE corrections.

bond, which maintains its *Z*-configuration generated from the initial outer-sphere nucleophilic attack of the indole on the gold-activated allenamide.

The final **M2(K)** product complex (the **4b** regioisomer) is 30.8 kcal mol⁻¹ more stable than reactants. In this complex the gold atom gets away from C β (C β –Au distance = 2.44 Å) and moves much closer to C α (2.37 Å), thus reactivating a η^2 coordination with the exocyclic double bond. Notably, the N–C2 distance (indole moiety) increases from 1.32 to 1.47 Å along the transformation **M1(K)**→**M2(K)**.

This points out the disappearance of the formal charge on the immonium ion (characterizing the indoleninic intermediate **M1(K)**) and the repositioning of the lone-pair on the nitrogen atom in **M2(K)**.

Also, it demonstrates the importance of the protecting group Boc that assists the cycloaddition process by displacing electron density from N–C(2).

Along Path(T) (thermodynamic pathway) the first transition state **TS1(T)** describes the nucleophilic attack of C2 on C γ (the new incipient C2–C γ bond is 2.14 Å) and corresponds again to the rate determining step of the process. **TS1(T)** is 7.6 kcal mol⁻¹ higher than **M0** (1.3 kcal mol⁻¹ above **TS1(K)**) and leads to **M1(T)**, the indoleninic dearomatized intermediate, where the new C2–C γ bond formation is completed (1.57 Å).

The dearomatization process occurring in the passage **M0**→**M1(T)** and involving the delocalization of the benzene π electrons on indole is evidenced by the gradual increase in the indole moiety of the C2–C3 (from 1.37 to 1.48 Å) and C4–C5 (from 1.41 to 1.44 Å) distances and a simultaneous shortening of C3–C4 bond (from 1.44 to 1.38 Å).

The transition state for the subsequent ring-closing step (transition state **TS2(T)**, 3.3 kcal mol⁻¹ above **TS2(K)**) has an intrinsic activation energy of 6.1 kcal mol⁻¹. The values of the computed bond lengths again indicate that the ring-closing process involves the C β –[Au] electrons. The stability of the resulting product **M2(T)** (34.3 kcal mol⁻¹ below reactants) can be reasonably ascribed to the restoring of the aromaticity of the indolinic ring. As observed for **M2(K)** the coordination mode of the gold cation [Au^I] again becomes η^2 . It is reasonable to believe that the energetic gap among these two adducts is due to the steric hindrance between the Boc and the oxazolinonic groups. In **M2(K)** these two groups are rather close, but this steric hindrance is partially cancelled in the thermodynamic adduct **M2(T)** (compare Figures S5 and S9 in the Supporting Information).

Comparison of the two reaction profiles clearly indicates that the two transition states for indole dearomatization (rate-determining step in both cases) are close enough (the two activation barriers differ by 1.3 kcal mol⁻¹) to explain why, when the reaction is performed at 0 °C, small amounts of the thermodynamic product are observed and only through a rigid kinetic control (–40 °C) it is possible to avoid the formation of the regioisomer **4b'**.

The energy difference between **TS1(K)** and **TS1(T)** can be plausibly ascribed to the different indole dearomatization ability associated with the attack of C(3) and C(2) on the allenamido carbon C γ . The energy cost is higher in the latter case where a loss of aromaticity of the entire system (also involving the benzene ring) occurs. Otherwise, when the attack proceeds from C(3) the loss of aromaticity is confined to the heterocyclic portion.

Enantioselective gold-catalyzed [2+2]-cycloaddition between indoles and electron-rich allenes

The enantioselective cycloaddition reactions^[20] involving indoles, represents a powerful tool for a direct access to stereochemically defined dearomatized indolyl-based scaffolds.^[21] As a matter of fact, several metal- and metal-free stereoselective methodologies have been developed with the site-selective functionalization of the C(2)- and C(3)-positions of the indole core.^[3] Interestingly, despite the enormous interest towards the development of efficient catalytic methodologies to polycyclic fused indolines, enantioselective protocols to access C(2)/(3)-

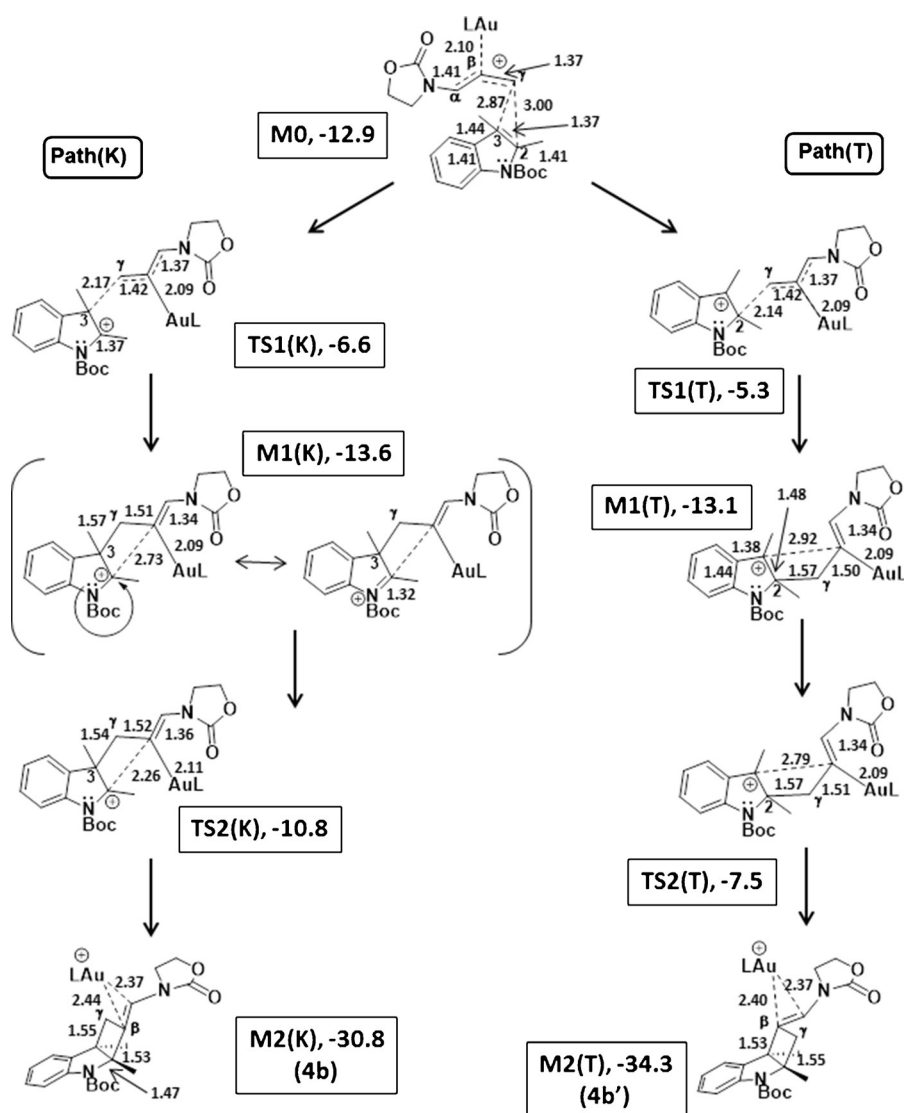


Figure 4. A schematic representation of the structures of the critical points located along Path(K) and Path(T). Energies [kcal mol⁻¹] are relative to reactants and include ZPE corrections. Bond lengths are given in Å.

cyclobutylindoline compounds were still unreported until our recent contribution on the stereoselective gold-catalyzed formal [2+2]-cycloaddition reaction.^[11]

In particular, the use of in situ formed (*R*)-DTBM-segphos(AuOTf)₂ (2.5–5.0 mol%) enabled the enantioselective preparation of tricyclic indoline scaffolds in straightforward manner by condensing a range of *N*-Boc-indoles and **2** (DCM, -60 °C).^[22]

A collection of results is depicted in Table 4. Here, excellent levels of regio-, diastereo- (d.r. > 20:1) and enantioselection (*ee* up to 98%) were obtained for differently substituted indoles. In particular, 2,3-annulated indoles carrying C5 and C7-membered rings worked particularly well providing methylenecyclobuta-indolines **1l–t** in enantiomeric excesses up to 99% (entries 7–14). Also, it appears that alkyl substituents were also tolerated at the C(2)/C(3)-sites (**1b–1j**), as well as EDGs and EWGs in the benzene ring C(5)-position. It is worth mentioning,

that the removal of the EWG group from the nitrogen causes a marked drop in the isolated yield (8%) but with similar enantiocontrol (91%, entry 1).

On the basis of these experimental evidences, the efficiency of the stereoselective gold-catalyzed intermolecular [2+2]-cycloaddition between aryloxyallenes and *N*-Boc indoles was investigated. Among the screened chiral ligands (see the Supporting Information), (*R*)-DTBM-segphos furnished the highest levels of chemical (61%) and optical (85%) yields (CH₂Cl₂, 0 °C, cat. loading = 2.5 mol%) in the model reaction (**3a** + **1b**) in combination with AgNTf₂ as the gold-activator.^[23] On the contrary, lower performances were recorded with different C1- and C2-symmetric chiral units.

Finally, the performances of the catalytic system in the case of aryloxyallenes were assessed by condensing several indoles with **3** under optimal conditions (Table 5). Aryloxyallenes **3** were generally found less reactive than that allenamide **2** in the enantioselective variant and higher reaction temperatures (i.e., 0 °C/–20 °C) were required in order to access synthetically acceptable reaction kinetics.

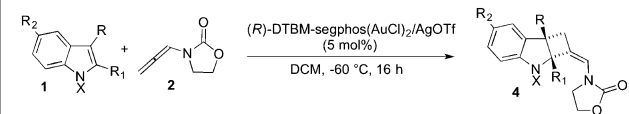
The enantioselectivity ranges from high (64%) to excellent (95%) with moderate to good

yield. Indoles featuring cyclic substituents at the C2/C3 carbon atoms (**1l,q**) and trimethyl-substituted indole **1e** (entry 5) were proved to be particularly competent.

Conclusions

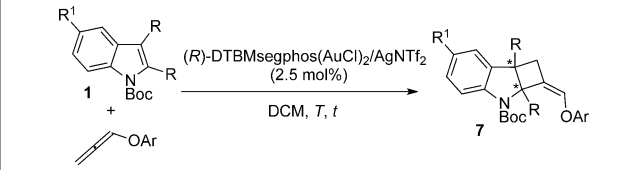
A comprehensive investigation of the gold-catalyzed dearomative cycloaddition reaction of indoles with electron-rich allenes is documented by means of experimental and computational tools.

Commercially available ([JohnPhosAu(NCMe)]SbF₆) showed competence in performing the chemo-, regio- and diastereoselective formal [2+2]-cycloaddition between a wide range of substrates under mild conditions. A portfolio of densely functionalized C(2),C(3)-fused cyclobutylindolines (**4/7**) is accessible in a straightforward manner. Additionally, the use of chiral C(2)-symmetric DTBM-segphos enabled the control of the ste-

Table 4. Enantioselective dearomative cycloaddition between indoles and **2**.^[a]


Run	R/R ¹ /R ² /X (1)	Yield 4 [%] ^[b]	ee 4 [%] ^[c]
1	Me/Me/H/H (1 a)	8	91
2	Me/Me/H/Boc (1 b)	95	93
3	Me/Me/H/Cbz (1 c)	60	96
4 ^d	Me/Me/Me/Boc (1 e)	90	81
5 ^d	Me/Me/OMe/Boc (1 f)	90	86
6	Me/Et/H/Boc (1 j)	72	92
7	-(CH ₂) ₃ -H/Boc (1 l)	96	94
8	-(CH ₂) ₃ -Me/Boc (1 m)	96	93
9	-(CH ₂) ₃ -OMe/Boc (1 n)	94	95
10	-(CH ₂) ₃ -Br/Boc (1 o)	55	94
11	-(CH ₂) ₅ -H/Boc (1 q)	95	98
12	-(CH ₂) ₅ -Me/Boc (1 r)	96	98
13	-(CH ₂) ₅ -OMe/Boc (1 s)	92	94
14	-(CH ₂) ₅ -Br/Boc (1 t)	41	99

[a] All the reactions were carried out under nitrogen atmosphere (**1/2** = 1.2:1). [b] Isolated yields after flash chromatography. [c] Determined by HPLC analysis with chiral column. Absolute configuration as reported in the Scheme of Table 4 (see ref. [11]). [d] Catalyst loading = 2.5 mol%.

Table 5. Gold-catalyzed enantioselective cycloaddition between indoles and **3**.^[a]


Run	R/R ¹ /R ² (1)	3	T [°C]/t [h]	Yield 7 [%] ^[b]	ee 7 [%] ^[c]
1	Me/Me/H (1 b)	3 a	0/4	61	(+)-85
2	Me/Me/H (1 b)	3 a	-20/6	32	(+)-95
3	Me/Me/Me (1 e)	3 a	-20/6	56	(+)-94
4	-(CH ₂) ₃ -H (1 l)	3 a	0/4	75	(+)-95
5	-(CH ₂) ₅ -H (1 q)	3 a	0/4	73	(+)-84
6	Me/Me/H (1 b)	3 f	0/16	74	(+)-64

[a] All the reactions were carried out under nitrogen atmosphere. [b] Isolated yields after flash chromatography. [c] Determined via HPLC analysis with chiral column. The absolute configuration of **7** was not determined.

reochemical profile of the dearomatization reaction in a convenient manner (ee up to 95% with aryloxyallenes and 99% with allenamide **2**).

Our DFT computations have clearly demonstrated that the mechanism for the formal gold-catalyzed cycloaddition among allenamide **2** and *N*-Boc-indole **1 b** proceeds through a polar non-concerted mechanism involving two kinetic steps. Two different reaction pathways (Path(K) and Path(T), both consisting of two steps) originate from an initial encounter complex and provide the two regioisomers experimentally observed, that is, **4 b** obtained under kinetic conditions and **4 b'** obtained under thermodynamic conditions. In both cases the first step is rate-

determining and corresponds to a dearomatization process. The ring closure occurring in the second step involves the heterolytic rupture of the σ [Au]–C β bond and not the electrons of the exocyclic C α =C β double bond, which maintains its original Z-configuration in agreement with the experiments.

The energy cost for the dearomatization process is higher along the thermodynamic pathway (attack from the C(2)-indole position) where the loss of aromaticity involves the entire system (indole and benzene ring). This cost decreases when the attack proceeds from C(3)- and the dearomatization is confined to the indole moiety. The energy difference between the two dearomatization transition states is not very large (about 1.3 kcal mol⁻¹). This explains why at 0 °C small amounts of the thermodynamic product **4 b'** are observed and only under severe kinetic conditions (-40 °C) it is possible to avoid the formation of this regioisomer.

Studies addressing the exploitation of the gold-catalyzed condensation of allenes with different aromatic compounds are currently under investigation in our laboratory.

Acknowledgements

University of Bologna and MIUR Rome are acknowledged for the financial support. Q.Q.Y. thanks the China Scholarship Council for financial support.

Keywords: allenamide • asymmetric catalysis • density functional calculations • gold • indole

- [1] a) P. J. Praveen, P. S. Parameswaran, M. S. Majik, *Synthesis* **2015**, 1827; b) N. Gupta, D. Goyal, *Chem. Het. Comp.* **2015**, 51, 4.
- [2] a) R. Dal Pozzo, *Chem. Soc. Rev.* **2015**, 44, 742; b) S. P. Roche, J.-J. Y. Tendoung, B. Trèguier, *Tetrahedron* **2015**, 71, 3549; and references therein; c) H. Wu, Y.-P. He, F. Shi, *Synthesis* **2015**, 1990.
- [3] For reviews on the topic: a) F. López Ortiz, M. J. Iglesias, I. Fernández, C. M. Andújar Sánchez, G. R. Gómez, *Chem. Rev.* **2007**, 107, 1580; b) L. Pouységu, D. Deffieux, S. Quideau, *Tetrahedron* **2010**, 66, 2235; c) S. P. Roche, J. A. Porco, Jr., *Angew. Chem. Int. Ed.* **2011**, 50, 4068; *Angew. Chem.* **2011**, 123, 4154; d) C.-X. Zhuo, W. Zhang, S.-L. You, *Angew. Chem. Int. Ed.* **2012**, 51, 12662; *Angew. Chem.* **2012**, 124, 12834; f) C. C. Loh, D. J. Enders, *Angew. Chem. Int. Ed.* **2012**, 51, 46; *Angew. Chem.* **2012**, 124, 46; g) C.-X. Zhuo, C. Zheng, S.-L. You, *Acc. Chem. Res.* **2014**, 47, 2558; h) Q. Ding, X. Zhou, R. Fan, *Org. Biomol. Chem.* **2014**, 12, 4807; i) W. Zi, Z. Zuo, D. Ma, *Acc. Chem. Res.* **2015**, 48, 702.
- [4] a) J. Barluenga, E. Tudela, A. Ballesteros, M. Tomás, *J. Am. Chem. Soc.* **2009**, 131, 2096; b) L. M. Repka, J. Ni, S. E. Reisman, *J. Am. Chem. Soc.* **2010**, 132, 14418; c) Y. Lian, L. Davies, *J. Am. Chem. Soc.* **2010**, 132, 440; d) G. Özüdü, T. Schubach, M. M. K. Boysen, *Org. Lett.* **2012**, 14, 4990; e) J. E. Spangler, H. M. L. Davies, *J. Am. Chem. Soc.* **2013**, 135, 6802; f) J. Huang, L. Zhao, Y. Liu, W. Cao, X. Wu, *Org. Lett.* **2013**, 15, 4338; g) H. Xiong, H. Xu, A. Liao, Z. Xie, Y. Tang, *J. Am. Chem. Soc.* **2013**, 135, 7851; h) H. Wang, S. E. Reisman, *Angew. Chem. Int. Ed.* **2014**, 53, 6206; *Angew. Chem.* **2014**, 126, 6320. For representative racemic examples, see: i) J. Zhang, Z. Chen, H.-H. Wu, J. Zhang, *Chem. Commun.* **2012**, 48, 1817; j) M. Kawano, T. Kiuchi, S. Negishi, H. Tanaka, T. Hoshikawa, J. Matsuo, H. Ishibashi, *Angew. Chem. Int. Ed.* **2013**, 52, 906; *Angew. Chem.* **2013**, 125, 940; k) H. Li, R. P. Hughes, J. Wu, *J. Am. Chem. Soc.* **2014**, 136, 6288.
- [5] a) G.-J. Duan, J.-B. Ling, W.-P. Wang, Y.-C. Luo, P.-F. Xu, *Chem. Commun.* **2013**, 49, 4625; b) W. R. Gutekunst, P. S. Baran, *J. Org. Chem.* **2014**, 79, 2430.
- [6] a) L. Zhang, *J. Am. Chem. Soc.* **2005**, 127, 16804; b) H. Faustino, P. Bernal, L. Castedo, F. López, J. L. Mascareñas, *Adv. Synth. Catal.* **2012**, 354, 1658.

- [7] D. Zhao, J. Zhang, Z. Xie, *J. Am. Chem. Soc.* **2015**, *137*, 9423.
- [8] a) N. Bongers, N. Krause, *Angew. Chem. Int. Ed.* **2008**, *47*, 2178; *Angew. Chem.* **2008**, *120*, 2208; b) R. A. Widenhoefer, *Chem. Eur. J.* **2008**, *14*, 5382; c) S. Sengupta, X. Shi, *ChemCatChem* **2010**, *2*, 609; d) R. L. La-Londe, W. E. Brenzovich, Jr., D. Benitez, E. Tkatchouk, K. Kelley, W. A. Goddard III, F. D. Toste, *Chem. Sci.* **2010**, *1*, 226; e) T. de Haro, C. Nevado, *Synthesis* **2011**, 2530; f) M. Bandini, *Chem. Soc. Rev.* **2011**, *40*, 1358; g) A. Pradal, P. Y. Toullec, V. Michelet, *Synthesis* **2011**, 1501; h) M. Rudolph, A. S. K. Hashmi, *Chem. Soc. Rev.* **2012**, *41*, 2448; i) M. Livendahl, A. M. Echavarren, *Chim. Oggi-Chem. Today* **2012**, *30*, 19; k) N. T. Patil, *Chem. Asian J.* **2012**, *7*, 2186; j) E. M. Barreiro, L. A. Adrio, K. K. Hii, J. B. Brazier, *Eur. J. Org. Chem.* **2013**, 1027; l) G. Cera, M. Bandini, *Isr. J. Chem.* **2013**, *53*, 848; m) G. Abbiati, F. Marinelli, E. Rossi, A. Arcadi, *Isr. J. Chem.* **2013**, *53*, 856; n) A. Fürstner, *Acc. Chem. Res.* **2014**, *47*, 925; o) C. Obradors, A. S. K. Echavarren, *Acc. Chem. Res.* **2014**, *47*, 902; p) Y.-M. Wang, D. Lackner, A. D. Toste, *Acc. Chem. Res.* **2014**, *47*, 889; q) W. Yang, A. S. K. Hashmi, *Chem. Soc. Rev.* **2014**, *43*, 2941; r) R. Dorel, R. A. Echavarren, *Chem. Rev.* **2015**, *115*, 9028; s) P. M. Barbour, L. J. Marholz, L. Chang, W. Xu, X. Wang, *Chem. Lett.* **2014**, *43*, 572.
- [9] For reviews on the topic: a) B. Alcaide, P. Almendros, C. Aragoncillo, *Chem. Soc. Rev.* **2010**, *39*, 783; b) F. López, J. L. Mascareñas, *Beilstein J. Org. Chem.* **2011**, *7*, 1075; c) F. López, J. L. Mascareñas, *Beilstein J. Org. Chem.* **2013**, *9*, 2250.
- [10] For a selected examples of gold-catalyzed [2+2]-cycloaddition reactions see: a) M. R. Luzung, P. Mauleón, F. D. Toste, *J. Am. Chem. Soc.* **2007**, *129*, 12402; b) H. Teller, S. Flügge, R. Goddard, A. Fürstner, *Angew. Chem. Int. Ed.* **2010**, *49*, 1949; *Angew. Chem.* **2010**, *122*, 1993; c) A. Z. González, D. Benitez, E. Tkatchouk, W. A. Goddard III, F. D. Toste, *J. Am. Chem. Soc.* **2011**, *133*, 5500; d) S. Suárez-Pantiga, C. Hernández-Díaz, E. Rubioand, J. M. González, *Angew. Chem. Int. Ed.* **2012**, *51*, 11552; *Angew. Chem.* **2012**, *124*, 11720; e) H. Teller, M. Corbet, L. Mantilli, G. Gopakumar, R. Goddard, W. Thiel, A. Fürstner, *J. Am. Chem. Soc.* **2012**, *134*, 15331; f) S. Suárez-Pantiga, C. Hernández-Díaz, M. Piedrafit, E. Rubio, J. M. González, *Adv. Synth. Catal.* **2012**, *354*, 1651; g) P. Maulón, *ChemCatChem* **2013**, *5*, 2149; h) R. E. M. Brooner, T. J. Brown, R. A. Widenhoefer, *Angew. Chem. Int. Ed.* **2013**, *52*, 6259; *Angew. Chem.* **2013**, *125*, 6379; i) X.-X. Li, L.-L. Zhu, W. Zhou, Z. Chen, *Org. Lett.* **2012**, *14*, 436; j) C. Obradors, D. Leboeuf, J. Aydin, A. M. Echavarren, *Org. Lett.* **2013**, *15*, 1576; k) H. Zheng, R. J. Felix, M. R. Gagné, *Org. Lett.* **2014**, *16*, 2272; l) A. Homs, C. Obradors, D. Leboeuf, A. M. Echavarren, *Adv. Synth. Catal.* **2014**, *356*, 221; m) Y. Su, Y. Zhang, N. G. Akhmedov, J. L. Petersen, X. Shi, *Org. Lett.* **2014**, *16*, 2478; n) D. Li, W. Rao, G. Liang Tay, B. J. Ayers, P. W. H. Chan, *J. Org. Chem.* **2014**, *79*, 11301; o) P. Bernal-Albert, H. Faustino, A. Gimeno, G. Asensio, J. L. Mascareñas, F. López, *Org. Lett.* **2014**, *16*, 6196; p) B. D. Robertson, R. E. M. Brooner, R. A. Widenhoefer, *Chem. Eur. J.* **2015**, *21*, 5714.
- [11] M. Jia, M. Monari, Q.-Q. Yang, M. Bandini, *Chem. Commun.* **2015**, *51*, 2320.
- [12] a) M. Bandini, A. Eichholzer, *Angew. Chem. Int. Ed.* **2009**, *48*, 9533; *Angew. Chem.* **2009**, *121*, 9697; b) M. Bandini, M. Monari, A. Romaniello, M. Tragni, *Chem. Eur. J.* **2010**, *16*, 14272; c) M. Bandini, A. Gualandi, M. Monari, A. Romaniello, D. Savoia, M. Tragni, *J. Organomet. Chem.* **2011**, *696*, 338; d) G. Cera, P. Crispino, M. Monari, M. Bandini, *Chem. Commun.* **2011**, *47*, 7803; e) G. Cera, S. Piscitelli, M. Chiarucci, G. Fabrizi, A. Gogiamani, R. S. Ramón, S. P. Nolan, M. Bandini, *Angew. Chem. Int. Ed.* **2012**, *51*, 9891; *Angew. Chem.* **2012**, *124*, 10029; f) G. Cera, M. Chiarucci, A. Mazzanti, M. Mancinelli, M. Bandini, *Org. Lett.* **2012**, *14*, 1350; g) M. Chiarucci, E. Matteucci, G. Cera, G. Fabrizi, M. Bandini, *Chem. Asian J.* **2013**, *8*, 1776; h) M. Chiarucci, R. Mocci, L.-D. Syntrivanis, G. Cera, A. Mazzanti, M. Bandini, *Angew. Chem. Int. Ed.* **2013**, *52*, 10850; *Angew. Chem.* **2013**, *125*, 11050; i) M. Jia, G. Cera, D. Perrotta, M. Monari, M. Bandini, *Chem. Eur. J.* **2014**, *20*, 9875; k) C. Romano, M. Jia, M. Monari, E. Manoni, M. Bandini, *Angew. Chem. Int. Ed.* **2014**, *53*, 13854; *Angew. Chem.* **2014**, *126*, 14074.
- [13] Other reaction media furnished lower isolated yields of **4a**: CH₃CN = 21 %, THF = 17 %, toluene = 15 %, DCE (80 °C) = 22 %.
- [14] a) C. Nieto-Oberhuber, S. López, A. M. Echavarren, *J. Am. Chem. Soc.* **2005**, *127*, 6178; b) E. Herrero-Gómez, C. N. Oberhuber, S. López, J. Benet-Buchholz, A. M. Echavarren, *Angew. Chem. Int. Ed.* **2006**, *45*, 5455; *Angew. Chem.* **2006**, *118*, 5581.
- [15] a) V. Pirovano, L. Decataldo, E. Rossi, R. Vicente, *Chem. Commun.* **2013**, *49*, 3594; b) Y. Wang, P. Zhang, Y. Liu, F. Xia, J. Zhang, *Chem. Sci.* **2015**, *6*, 5564.
- [16] Lower temperatures caused a significant drop in the isolated yield.
- [17] R. Zimmer, H.-U. Reissig, *Chem. Soc. Rev.* **2014**, *43*, 2888, and references therein.
- [18] Electron-“neutral” and electron-poor arenes were employed in order to guarantee synthetically acceptable stability of the corresponding alenes. Aryloxallenes featuring electron-rich arenes proved to rapidly self-polymerize even at low temperatures and turned out to be unsuitable for the present protocol.
- [19] S. Montserrat, H. Faustino, A. Lledós, J. L. Mascareñas, F. López, G. Ujaque, *Chem. Eur. J.* **2013**, *19*, 15248.
- [20] Y. Xu, M. L. Conner, M. K. Brown, *Angew. Chem. Int. Ed.* **2015**, *54*, 11918; *Angew. Chem.* **2015**, *127*, 12086.
- [21] For recent examples of stereoselective dearomatization of indoles see: a) O. Lozano, G. Blessley, T. Martínez del Campo, A. L. Thompson, G. T. Giuffredi, M. Bettati, M. Walker, R. Borman, V. Gouverneur, *Angew. Chem. Int. Ed.* **2011**, *50*, 8105; *Angew. Chem.* **2011**, *123*, 8255; b) Q. Cai, C. Zheng, J.-W. Zhang, S.-L. You, *Angew. Chem. Int. Ed.* **2011**, *50*, 8665; *Angew. Chem.* **2011**, *123*, 8824; c) Q. Cai, S.-L. You, *Org. Lett.* **2012**, *14*, 3040; d) Q. Cai, C. Liu, X.-W. Liang, S.-L. You, *Org. Lett.* **2012**, *14*, 4588; e) W. Xie, G. Jiang, H. Liu, J. Hu, X. Pan, H. Zhang, X. Wan, Y. Lai, D. Ma, *Angew. Chem. Int. Ed.* **2013**, *52*, 12924; *Angew. Chem.* **2013**, *125*, 13162; f) M. E. Kieffer, K. V. Chuang, S. E. Reisman, *J. Am. Chem. Soc.* **2013**, *135*, 5557; g) H. Liu, G. Jiang, X. Pan, X. Wan, Y. Lai, D. Ma, W. Xie, *Org. Lett.* **2014**, *16*, 1908; h) Y.-C. Zhang, J.-J. Zhao, F. Jiang, S.-B. Sun, F. Shi, *Angew. Chem. Int. Ed.* **2014**, *53*, 13912; *Angew. Chem.* **2014**, *126*, 14132; i) L. Han, C. Liu, W. Zhang, X.-X. Shi, S.-L. You, *Chem. Commun.* **2014**, *50*, 1231; j) W. Zi, H. Wu, F. D. Toste, *J. Am. Chem. Soc.* **2015**, *137*, 3225. See also ref. [15b].
- [22] Attempts to synthesize the thermodynamic analogous (**4b'**) in stereochemical defined manner were carried out in refluxing conditions. However, substantial decomposition of the starting allenamide was observed.
- [23] a) M. Jia, M. Bandini, *ACS Catal.* **2015**, *5*, 1638; b) L. Rocchigiani, M. Jia, M. Bandini, A. Macchioni, *ACS Catal.* **2015**, *5*, 3911; c) B. Ranieri, I. Escofet, A. E. Echavarren, *Org. Biomol. Chem.* **2015**, *13*, 7103.